

DOI:10.13476/j.cnki.nsbddqk.2021.0046

束龙仓,张曼琦,李虎,等.两种典型边界条件下的趵突泉泉域水均衡分析[J].南水北调与水利科技(中英文),2021,19(3):427-436,445. SHU L C,ZHANG M Q,LI H,et al. Analysis of water balance in Baotu Spring basin under two typical boundary conditions[J]. South-to-North Water Transfers and Water Science & Technology,2021,19(3):427-436,445. (in Chinese)

两种典型边界条件下的趵突泉泉域水均衡分析

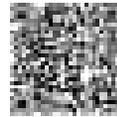
束龙仓¹,张曼琦¹,李虎²,倪寒茜¹,武朝军²,陈媛¹,王小博¹,余亚飞¹

(1. 河海大学水文水资源学院,南京 210098; 2. 济南轨道交通集团有限公司,济南 250014)

摘要:以趵突泉泉域为例,采用水量均衡法和数值法两种方法,对两种典型边界条件下的水均衡进行计算,结果表明:在对断裂-分水岭边界确定的趵突泉泉域进行数值模拟时,需要充分考虑地表水与地下水之间密切的水力联系以及两者之间的转化关系,对降水入渗补给量进行合理折算,提高水均衡计算的准确性。水量均衡法结果表明断裂边界泉域与断裂-分水岭边界泉域的均衡差分别为 3 626.0 万 m³/a 和 3 061.4 万 m³/a;而利用数值法,均衡差分别为 4 467.1 万 m³/a 和 3 699.6 万 m³/a。研究结果为趵突泉泉域水资源评价工作提供了科学依据。

关键词:岩溶泉域;边界条件;水均衡;数值法

中图分类号:TV213 文献标志码:A 开放科学(资源服务)标志码(OSID):



岩溶区地下水资源的合理开发、利用、管理和保护已成为摆在人们面前的一个时代问题^[1-2]。对岩溶区地下水均衡情况的准确认识能为科学评价地下水资源提供技术保证。水量均衡法和数值法是当前应用最为广泛的两种地下水均衡研究方法^[3-4]。岩溶区水均衡情况的研究需要确定岩溶水系统的边界位置及水文地质性质,岩溶区岩性和构造的高度复杂性^[5]使其成为当前研究的热点与难点。学者们^[6-11]运用系统理论、水动力学、水化学、地球物理勘探等方法对岩溶区地下水系统的边界展开研究。

济南是著名的“泉城”,但由于城市的快速发展^[12]及地下水开采量的增加,历史上泉水经常发生断流。近些年,济南开展的保泉工作取得一定成效^[13],使趵突泉于 2003 年 9 月 6 日复流至今,但每年的 5、6 月份,泉水依旧存在着断流的风险^[14]。目前关于趵突泉泉域的东、西边界存在两种不同的观点,泉域边界位置和性质不清,泉水保护工作很难具有针对性^[15]。因此,对两种边界条件下泉域的水均

衡展开研究,为趵突泉泉域地下水资源的准确评价、合理利用与科学保护提供理论基础。

1 趵突泉泉域边界争议

趵突泉泉域东西边界的确定一直是学界研究的重点问题。部分学者^[16-17]认为马山断裂将趵突泉泉域和长孝岩溶水系统切割为 2 个相对独立的水文地质单元,东坞断裂将趵突泉泉域和白泉泉域切割为 2 个相对独立的水文地质单元,泉域边界见图 1(a)。为了便于描述,后文将此边界确定的泉域范围称为断裂边界泉域。

近年来有学者^[18-20]对断裂边界提出质疑,认为断裂边界是基于早期的勘探资料确定的,但大量、长期持续开采改变了地下水流动场,仍将整个马山断裂、东坞断裂作为边界不太合理。孙斌等^[18]从岩溶水系统的概念出发对济南地区岩溶地下水系统进行划分,依据相邻泉域间的水力联系,认为泉域的西部边界为:在岗辛以南为地表分水岭,岗辛以北为马山断裂;泉域的东部边界为:石岭以南为

收稿日期:2020-12-17 修回日期:2021-04-02 网络出版时间:2021-04-08

网络出版地址:https://kns.cnki.net/kcms/detail/13.1430.TV.20210408.1010.002.html

基金项目:国家自然科学基金(41172203)

作者简介:束龙仓(1964—),男,安徽无为,人,教授,博士生导师,主要从事地下水资源评价与管理研究。E-mail:lcsu@hhu.edu.cn

地表分水岭,石岭以北至徐家庄为东坞断裂。提出趵突泉泉域东、西边界均为断裂-分水岭,泉域范围

见图 1(b)。后文称此边界确定的泉域范围为断裂-分水岭边界泉域。

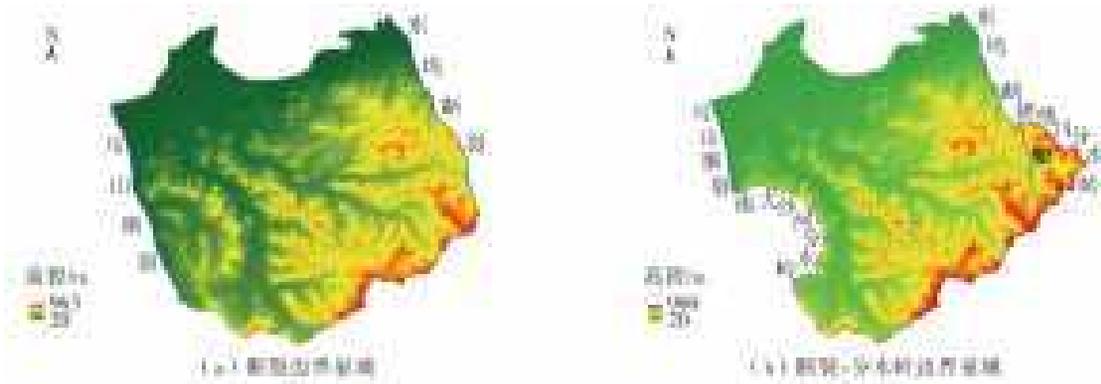


图 1 两种边界示意图

Fig. 1 Two kinds of boundary diagrams

2 断裂边界性质

2.1 马山断裂

(1)地层岩性。马山断裂两侧地层有明显错动,岩性有较大差异,水理性质也有较大差别。根据断裂两侧岩性可以将断裂分为 4 段,主要岩性见表 1。岗辛以南段泰山群变质岩在风化层下坚硬密实不透水,故该段为地层阻水。岗辛-孙庄段东侧地层地下

岩溶不发育,透水性差,富水性弱,特别是崮山组、炒米店组下部地层,为相对隔水地层,断层西侧岩溶发育、透性好,故此段东侧的地层阻水。孙庄-老屯段断层两侧,岩性相同,富水性均较好,但两侧岩溶含水层发育的不均一,主要岩溶含水段标高不同,东侧较西侧高,断层东侧的地层对西侧的岩溶水含水层起相对阻水作用,故此段具弱透水性。老屯-前隆段两侧岩溶均发育,富水性好,此段透水。

表 1 马山断裂东西两侧岩性

Tab. 1 Lithology of east and west sides of Mashan fault

位置	岩性	透水性
岗辛以南段	东盘 泰山群变质岩 西盘 寒武系灰岩、页岩	阻水
岗辛-孙庄段	东盘 寒武系张夏组、崮山组、炒米店组和奥陶系下统三山子组白云岩 西盘 奥陶系灰岩,岩溶发育、透水性好	阻水
孙庄-老屯段	东盘 奥陶系马家沟群的灰岩 西盘 奥陶系马家沟群的灰岩	弱透水
老屯-前隆段	东盘 奥陶系马家沟群五阳山组灰岩 西盘 奥陶系马家沟群五阳山组、阁庄组和八陡组灰岩	透水

(2)流场对比。马山断裂两侧 1985 年 10 月及 2011 年 12 月的水位图,由图 2 可以发现:在长清以北地区,马山断裂两侧等水位线连续,东西两侧水力联系密切;长清以南地区,马山断裂两侧等水位线断开,西侧等水位线稀疏,东侧等水位线密集,说明此段马山断裂两侧水力联系变弱,断裂相对阻水。根据流场图可以得知,马山断裂为一相对阻水的断层,仅在断裂北段透水性良好。

2.2 东坞断裂

(1)地层岩性。根据钻孔资料,东坞断裂两侧岩性见表 2。黄寨以南段两盘地层倾向相背,由于

地处山区,地下水径流方向为北西,区域地下水流线基本平行断裂线,不会有穿越断裂的径流,形成地层阻水。黄寨-刘志远段此段顶部地层隔水,由于是晚期压性断层,断裂带内存在寒武系崮山组、炒米店组地层,受挤压后形成断层泥等物质起阻水作用。因此,该段断层阻水。刘志远-徐家庄段断裂两侧岩溶发育不均一,导致此段断层阻水。从徐家庄至大水坡村由于有岩浆岩穿插,奥陶系地层被分割为互不连续的两部分,断裂东侧中奥陶系灰岩地下水与西侧深部的下奥陶系灰岩局部有一定的水力联系,此段具有弱透水性。

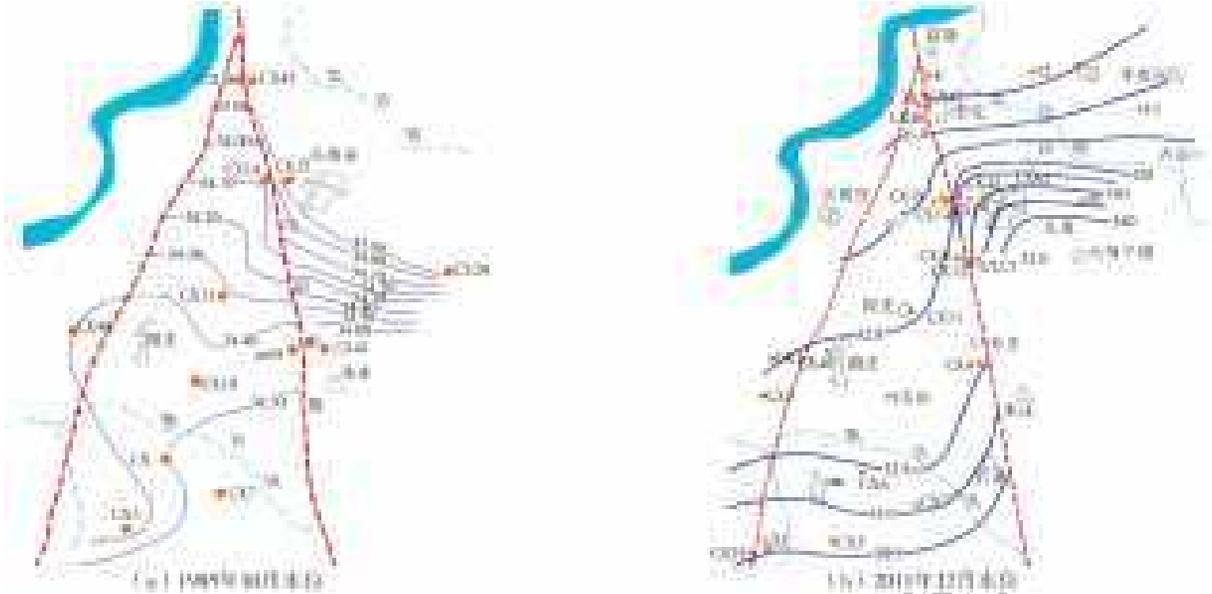


图2 马山断裂两侧流场^[21]

Fig. 2 Flow field diagram on both sides of Mashan fault

表2 东坞断裂东西两侧岩性

Tab. 2 Lithology of east and west sides of Dongwu fault

位置		岩性	透水性
黄寨以南段	东盘	寒武系馒头组和泰山群变质岩不透水地层	阻水
	西盘	寒武系张夏组和炒米店组地层	
黄寨-刘志远段	东盘	顶部为寒武系炒米店组,断裂带内存在寒武系崮山组、炒米店组地层	阻水
	西盘	顶部为奥陶系马家沟群东黄山组,断裂带内存在寒武系崮山组、炒米店组地层	
刘志远-徐家庄段	东盘	奥陶系灰岩地层	阻水
	西盘	奥陶系灰岩地层	
徐家庄-大水坡段	东盘	岩浆岩穿插奥陶系地层	弱透水性
	西盘	岩浆岩穿插奥陶系地层	

(2)流场对比。1963年泉域内地下水开发程度较低,人为影响较小,且是丰水年份,该年的地下水动态能真实反映趵突泉泉域岩溶水的补给条件,由图3(a)可知1963年11月东坞断裂两侧水位不一致。20世纪60年代以后随着东坞断裂附近地下水的大量开采,地下水流场发生变化,由图3(b)可知断裂两侧地下水位等值线间断不连续,断裂西侧漏斗区水位标高15 m左右,断裂东侧漏斗区水位标高17 m左右,在徐家庄—济南铁厂一段,断裂西盘为济南铁厂和炼油厂的供水水源地,西盘的地下水降落漏斗透过断裂影响东盘,两盘间存在一定的水头差,断裂东侧水位高于西侧,证明该段透水。从整体分析,东坞断裂的阻水性较为明显,仅徐家庄-大水坡段具弱透水性。

3 基于数值模拟的边界水量交换研究

正确分析分水岭与断裂包围的区域“三水”(大气降水、地表水、地下水)转化情况,可以提高两种方

法水均衡计算的准确性,因此以马山断裂与南大沙河分水岭包围区域为例对该区域的三水转化情况展开研究。

图4(a)表明该区域地质构造以及大气降水的去向,由图可知,大气降水进入断裂-分水岭区域后,一部分转化为地表径流(surface runoff, SR)穿过马山断裂,一部分入渗补给地下水。南大沙河流域的大气降水转化的地表径流、孔隙水(porous subsurface runoff, PSSR)将穿过马山断裂流出趵突泉泉域。只有由南大沙河谷区孔隙水下渗补给的裂隙岩溶水(karstic subsurface runoff, KSSR)才能在寒武系单斜地层控制下流入该泉域。泉域东侧的东坞断裂与锦绣川分水岭所构成的区域也存在类似的水量转化过程。

将上述区域地质构造简化并通过FEFLOW建立数值模型(图4(b)),两峰形成分水岭,山谷对应南大沙河,侧面对应马山断裂。根据趵突泉泉域内钻孔资料,进行含水层概化以及参数设置。模型中从上到下

依次为土壤层(I)、孔隙含水层(II)及岩溶含水层(III), 水平渗透系数 K_h 分别设置为 5、15、10 m/d, 垂直渗透系数 K_v 分别设置为 1.0、2.0、0.5 m/d。依据研究区的地质构造和水文过程设置唯一补给源即降水; 由于河谷内覆盖的第四系与邻域存在水量交换, 所以在河谷地带和孔隙含水层设有渗流边界; 模拟分水岭范围内降水转化为地表径流、孔隙水、岩溶水的过

程。模型四周及底部基本为隔水边界, 在土壤层的河谷地带两侧、孔隙层及岩溶层底部下游位置采用一类水头边界中的 Seepage Face 设置出流边界以计算出流量, 唯一补给来源为山谷降水, 采用 In/outflow on top/bottom 模块进行赋值。此模型可以研究在不同降水强度下区域内的降水转化为地表径流、孔隙地下水径流与岩溶地下水径流的规律。

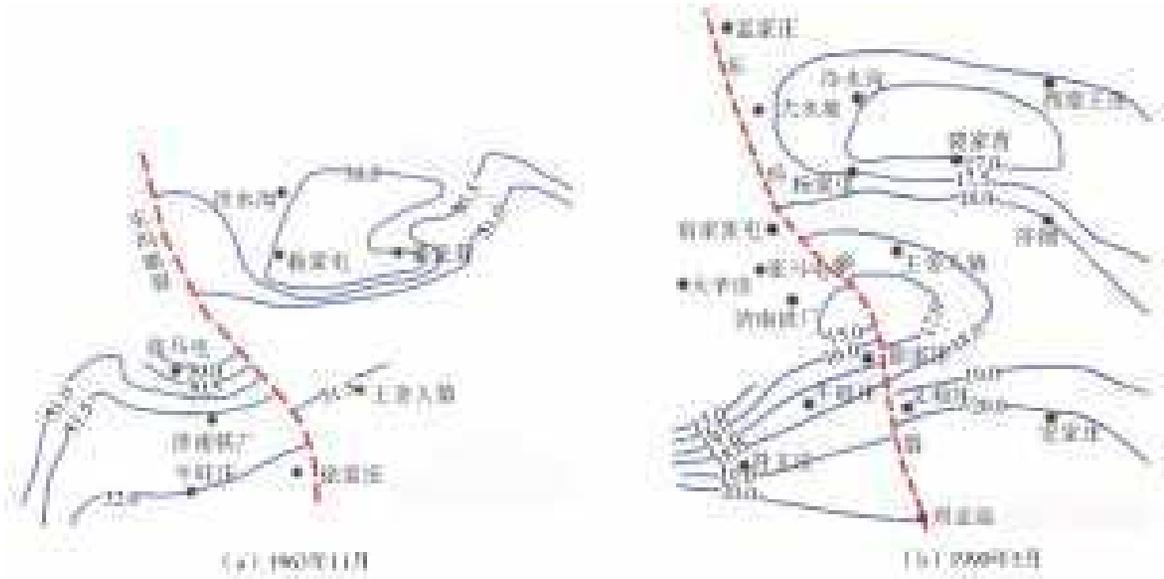


图 3 东坞断裂附近流场^[21]
Fig. 3 Flow field diagram near Dongwu fault

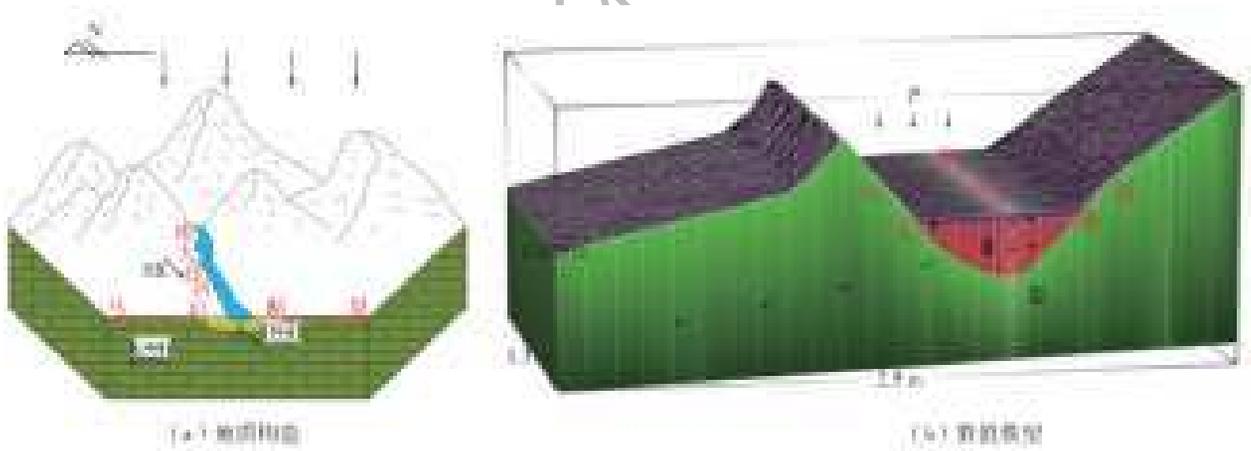


图 4 地质构造与数值模型示意图
Fig. 4 Numerical model schematic diagram

设置 15 组不同降水量进行模拟, 运行完成后利用水均衡分析工具计算各层出流量并计算占比, 计算结果见表 3。

由表 3 可以得知: 随着降雨强度的增加, 河道排泄量及孔隙水出流量都随之增加, 但是裂隙水出流量呈现先增后减的趋势, 变化幅度较小; 而降水量转化为河道排泄量的占比与降水强度呈正相关, 孔隙水出流量和裂隙水出流量的占比与降水强度呈负相关。整体来看, 孔隙水出流量占比较

为稳定, 约在 50% 左右。根据 15 组模拟数据, 绘制河道排泄量占比 R_{SR} (SR 与降水量的比值) 与降水量 P 的关系图以及裂隙水出流量占比 R_{KSSR} (KSSR 与降水量的比值) 与降水量 P 的关系图, 分别见图 5、6。

由图 5、6 拟合结果, 在对该区域进行水均衡分析时, 河道排泄量占比通过 $R_{SR} = 33.967 \ln P - 14.728$ 折算, 裂隙水出流量占比通过 $R_{KSSR} = -30.52 \ln P + 59.941$ 折算。

表 3 降水入渗转化结果

Tab. 3 Precipitation infiltration transformation results

模拟 编号	降水量 P		河道排泄量 R_{SR}		孔隙水出流量 R_{PSSR}		岩溶水出流量 R_{KSSR}	
	数值/ $(\text{m}^3 \cdot \text{d}^{-1})$	比例/%	数值/ $(\text{m}^3 \cdot \text{d}^{-1})$	比例/%	数值/ $(\text{m}^3 \cdot \text{d}^{-1})$	比例/%	数值/ $(\text{m}^3 \cdot \text{d}^{-1})$	比例/%
1	1.79	100	0.09	5.03	0.94	52.51	0.760	42.46
2	1.88	100	0.13	6.91	0.99	52.66	0.769	40.90
3	1.98	100	0.16	8.08	1.04	52.53	0.775	39.14
4	2.07	100	0.20	9.66	1.08	52.17	0.779	37.63
5	2.26	100	0.31	13.72	1.17	51.77	0.783	34.65
6	2.45	100	0.40	16.33	1.26	51.43	0.787	32.12
7	2.64	100	0.50	18.94	1.35	51.14	0.79	29.92
8	2.83	100	0.59	20.85	1.44	50.88	0.795	28.09
9	3.20	100	0.78	24.38	1.63	50.94	0.794	24.81
10	3.58	100	0.99	27.65	1.82	50.84	0.769	21.48
11	3.77	100	1.10	29.18	1.92	50.93	0.756	20.05
12	4.16	100	1.31	31.49	2.12	50.96	0.723	17.38
13	4.53	100	1.71	37.75	2.25	49.67	0.575	12.69
14	4.91	100	1.97	40.12	2.41	49.08	0.537	10.94
15	5.23	100	2.22	42.45	2.56	48.95	0.504	9.64

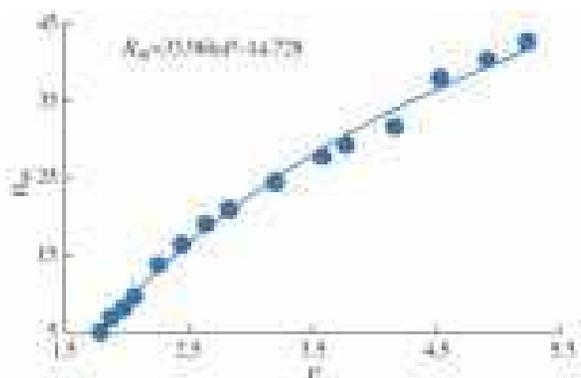


图 5 河道排泄量占比趋势

Fig. 5 Trend of proportion of river excretion

期确定为 2012 年 10 月至 2013 年 9 月。趵突泉泉域地下水水流系统主要补给来源包括大气降水入渗补给 $Q_{雨渗}$ 、灌溉回渗补给 $Q_{灌渗}$ 、河道渗漏补给 $Q_{河渗}$ 、地下水侧向补给 $Q_{侧补}$ 以及人工回灌补给 $Q_{回灌}$ 。主要排泄项包括人工开采 $Q_{开采}$ 、地下水侧向排泄 $Q_{侧排}$ 、泉水排泄 $Q_{泉排}$ (蒸发可以忽略不计)。总补给量与排泄量之差即为泉域内储存量的变化量 $\Delta\omega_{泉域}$, 也即泉域的均衡差。收集相关资料, 分项计算各均衡项。最终, 将各均衡项代入均衡方程, 计算均衡差。趵突泉泉域的均衡方程为

$$\Delta\omega_{泉域} = Q_{雨渗} + Q_{灌渗} + Q_{河渗} + Q_{侧补} + Q_{回灌} - Q_{开采} - Q_{侧排} - Q_{泉排} \quad (1)$$

其中, 大气降水入渗补给 ($Q_{雨渗}$) 根据收集的 15 个气象站所记录的降水数据, 根据《山东省济南市保泉供水地质勘探水质模型报告》《济南市城市总体规划(2011—2020 年)》给出的城市建设绿化覆盖率与城市住宅区建设方式确定降水入渗补给系数的取值。在断裂-分水岭包围区域, 利用第 3 节的结论进行折算。

泉域内地下水通过东西边界获得泉域外地下水侧向补给的断面有以下两条。(1) 东坞断裂北段, 根据《山东省济南市白泉-武家水源地供水水文地质勘探报告》确定地下水侧向补给量为 $292.0 \text{ 万 m}^3/\text{a}$ 。(2) 马山断裂长清以北段, 地下水侧向补给量通过公式 $Q_{侧补} = TIB$ 计算, 其中: T 为导水系数, m^2/d , 根据马山断裂两侧 CX45、CX46 号孔抽水试验确定取

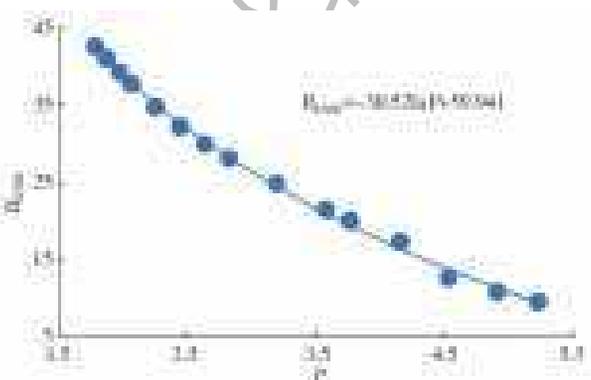


图 6 裂隙水出流量占比趋势

Fig. 6 Trend of proportion of fissure water outflow

4 不同边界条件下的水均衡分析

4.1 水量均衡法

研究的均衡区即两种边界所确定的范围。均衡

值为 20 000 m²/d; I 为水力坡度, 根据水位等值线图计算为 0.24‰; B 为过水断面宽度, m, 依据资料与实地考察, 取 8 700 m。

泉域内地下水的排泄断面共两条: (1) 从长清县城北的小房庄到市郊睦里庄, 断面长 19 500 m; (2) 西起王府庄, 东到担山屯南, 断面长 6 250 m。导水系数根据断面附近 J25、KA3 钻孔的实际抽水资料, 采用图解法计算, 平均 2 000 m²/d。水力坡度由等水位线图计算确定, 平均水力坡度 0.53‰。地下水侧向排泄量通过公式 $Q_{\text{侧排}} = TIB$ 计算。

根据统计的两种泉域内农田面积与农业灌溉开采量, 入渗系数取 0.15, 计算得到灌溉回渗补给量 ($Q_{\text{灌渗}}$)。河道渗漏量 ($Q_{\text{河渗}}$) 根据河道实测资料与现场勘测的河道现状计算。回灌量、开采量、排泄量依据统计资料得到。

4.2 数值法

4.2.1 水文地质概念模型

(1) 边界条件^[12,15,17]。两种泉域南北边界无差别。南部以平阴-东平的地下(地表)分水岭、孝直断裂以及寒武系中统张夏组底界面为界, 概化为隔水边界; 北部以奥陶系灰岩顶板埋深 600 m 线为界, 概化为隔水边界。断裂边界泉域的东部边界为东坞断裂, 依据第 2 节的结论, 徐家庄-大水坡段设为透水边界, 徐家庄以南设为隔水边界。断裂边界泉域的西部边界为马山断裂, 其中孙庄-前隆段透水, 孙庄以南阻水。断裂-分水岭边界泉域的东部边界以夏家村为界, 分为上下两段, 上段为东坞断裂, 下段为锦绣川分水岭, 其中, 徐家庄-大水坡段设为透水边界, 徐家庄-夏家村段为隔水边界, 分水岭部分为隔水边界。西部边界以岗辛为界分为上下两段, 上段为马山断裂, 下段为南大沙河分水岭, 其中, 孙庄-前隆段透水, 孙庄-岗辛段为隔水边界, 分水岭部分为隔水边界。

(2) 含水层概化^[12,15,17]。泉域南部碳酸盐岩裸露区为潜水含水层, 泉域北部岩溶覆盖区为承压含水层。模拟区内岩溶水垂向速度分量很小, 可忽略不计。潜水与承压水水流均符合达西流, 可概化为二维非稳定流。

4.2.2 数学模型

根据上述水文地质概念模型, 建立相应的数学模型如式(2)所示。

$$\begin{cases} \frac{\partial}{\partial x} \left(T \frac{\partial H}{\partial x} \right) + \frac{\partial}{\partial y} \left(T \frac{\partial H}{\partial y} \right) + W = E \frac{\partial H}{\partial t}, (x, y) \in D \\ T \frac{\partial H(x, y)}{\partial n} \Big|_{\Gamma_2} = q(x, y, t), (x, y) \in \Gamma_2 \\ H(x, y, t) \Big|_{t=0} = H_0(x, y), (x, y) \in D \end{cases} \quad (2)$$

其中:

$$T = \begin{cases} T & \text{承压区} \\ K(H-B) & \text{潜水区} \end{cases} \quad (3)$$

$$E = \begin{cases} \mu^* & \text{承压区} \\ \mu & \text{潜水区} \end{cases} \quad (4)$$

式中: D 为地下水渗流区域; W 为单位时间从单位体积含水层中流出的水量, m³; K 为渗透系数, m/d; T 导水系数, m²/d; μ 为潜水含水层给水度; μ^* 为承压含水层弹性释水系数; B 为潜水含水层底板高程, m; n 为二类流量边界外法线方向; Γ_2 为二类流量边界; q 为边界上流入或流出的单宽流量, m²。

4.2.3 数值模型建立

选用 FEFLOW 软件, 分别建立图 1 中两种东西边界条件下泉域地下水流的数值模型。在 FEFLOW 提供的 4 种网格剖分方法中, Triangle 法有利于模型计算求解的稳定, 采用该法进行网格剖分。将地下水位数据在剖分的网格上进行空间插值, 作为模型计算的初始条件。采用 2012 年 10 月 1 日统测的承压水水位作为模拟的初始流场。根据趵突泉泉域实际水文地质条件, 对各含水层分别进行水文地质参数分区。岩溶含水层的水文地质参数分区及赋值见表 4、图 7。

表 4 岩溶含水层水文地质参数赋值
Tab. 4 Hydrogeological parameters of karst aquifer

分区编号	水平渗透系数 $K_h / (m \cdot d^{-1})$	垂直渗透系数 $K_v / (m \cdot d^{-1})$	贮水率
1	50.0	5.00	0.000 10
2	5.0	0.50	0.000 10
3	0.1	0.01	0.000 10
4	100.0	10.00	0.000 50
5	50.0	5.00	0.100 00
6	30.0	3.00	0.006 00
7	5.0	0.50	0.050 00
8	50.0	5.00	0.000 01
9	0.1	0.01	0.000 10
10	10.0	1.00	0.100 00
11	0.1	0.01	0.020 00

结合以上边界条件、含水层概化情况以及水文地质参数分区等, 建立数值模型见图 8。

泉域内 8 个观测井, 其位置见图 9。其中, 3 号与 65 号观测井为潜水井, 其余均为承压水观测井。通过观测井的水位观测数据调整泉域水文地质参数取值。泉域内典型观测点趵突泉与黑虎泉的水位拟合结果见图 10。观测井地下水位的实际观测值与模拟计算的拟合误差小于拟合计算期间内水

位变化幅度的 10%,数值模型拟合较好,水均衡计算结果可靠。

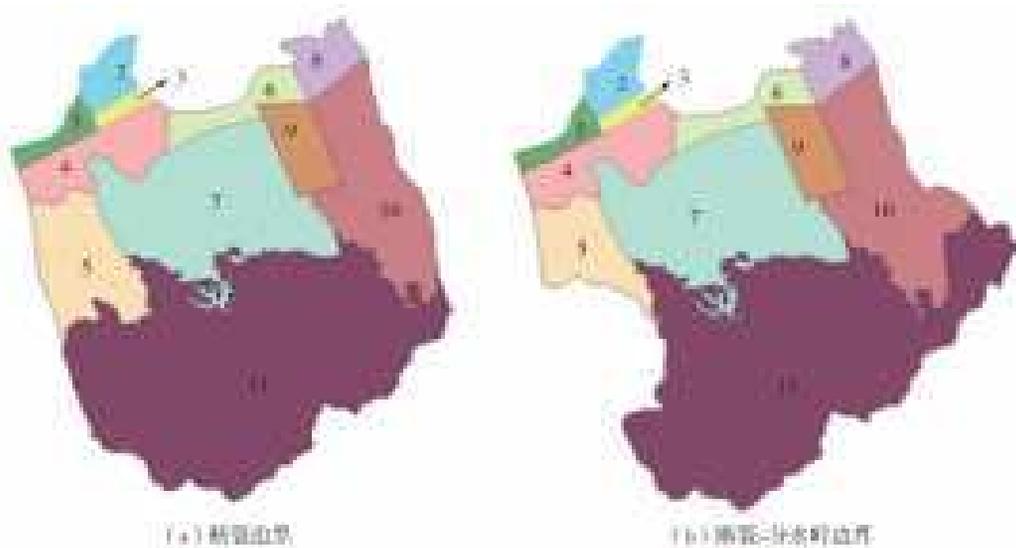


图 7 岩溶含水层水文地质参数分区

Fig. 7 Division diagram of hydrogeological parameters of karst aquifer

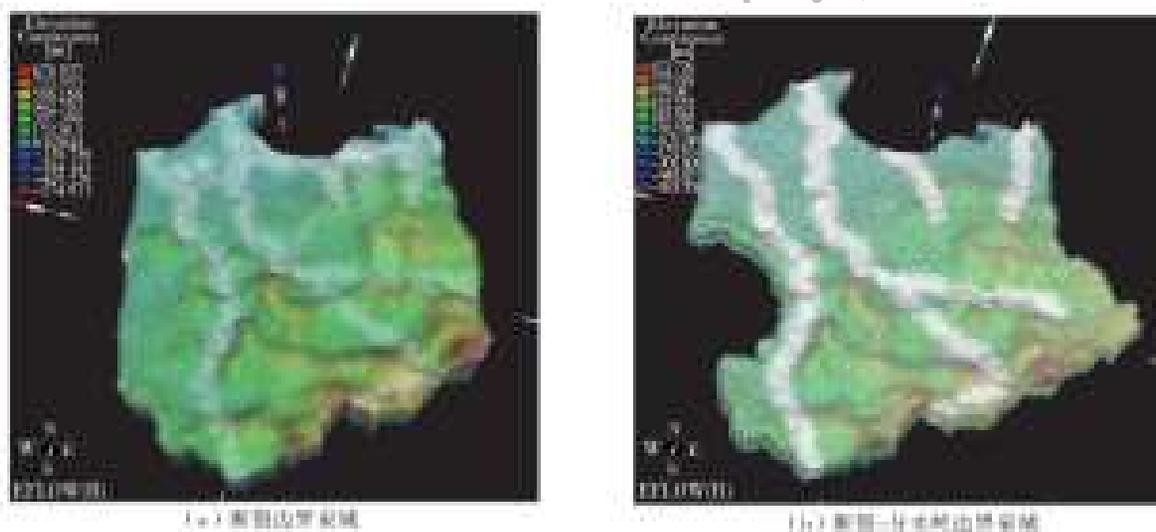


图 8 不同边界的数学模型

Fig. 8 Schematic diagram of mathematical models with different boundaries



图 9 监测井位置

Fig. 9 Diagram of monitoring well location

4.3 计算结果

采用水量均衡法和数值法分别计算两种边界泉域的水均衡情况,结果见表 5。根据计算结果,在两种边界条件下,水量均衡法与数值法计算的水均衡结果都较为接近,两种方法相互验证,表明水均衡计算结果的可靠性和精确性。

经过对比分析可以发现,在两种边界情况下,趵突泉泉域均处于正均衡状态(即泉域地下水的补给量大于排泄量)。根据水量均衡法计算结果,断裂边界泉域的补给量、排泄量以及均衡差分别比断裂分水岭边界泉域大 902.2 万、337.6 万和 564.6 万 m^3/a 。根据数值法计算结果,两种边界泉域的补给量、排泄量以及均衡差的差值分别为 1 210.8 万、

443.3 万和 767.5 万 m^3/a 。两种计算方法的结果虽然数值上有差异,但均表明断裂边界泉域

补给量、排泄量以及均衡差均大于断裂-分水岭边界泉域。

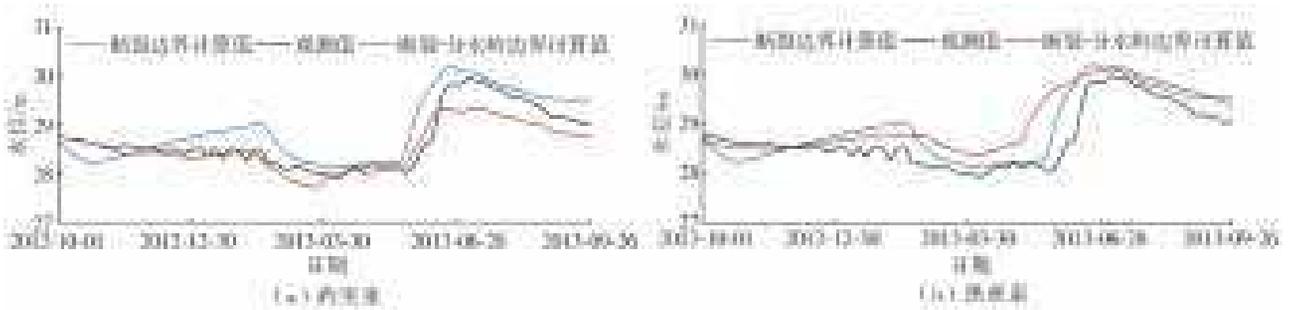


图 10 水位动态拟合结果

Fig. 10 Results of dynamic water level fitting

表 5 水均衡计算
Tab. 5 Water balance calculation

		单位:万 m^3/a		
计算方法	断裂边界泉域	断裂-分水岭边界泉域	差值	
水量均衡法	补给量	21 205.8	20 303.6	902.2
	排泄量	17 579.8	17 242.2	337.6
	均衡差	3 626.0	3 061.4	564.6
数值法	补给量	20 645.5	19 434.7	1 210.8
	排泄量	16 178.4	15 735.1	443.3
	均衡差	4 467.1	3 699.6	767.5

两种泉域的差异在于,断裂-分水岭边界泉域比断裂边界泉域少了西部马山断裂与南大沙河分水岭中间区域(简称西部区域),但东部多出东坞断裂与锦绣川分水岭中间区域(简称东部区域)。由图 1 可知,东西区域的地表高程差异较大,东部区域位于山区,高程较高且起伏大,西部区域高程较低,起伏较小。两个区域的地层岩性、地质构造均有差别,因此两种泉域的水均衡情况有所不同。然而,从面积变化看,断裂边界泉域面积(1 795.55 km^2)仅比断裂-分水岭边界泉域(1 713.28 km^2)大 88.27 km^2 ,仅约为前者泉域总面积的 1/18,面积差别较小,因此两种泉域水均衡情况差别较小。

5 结 论

利用数值法探讨了断裂-分水岭边界的水量交换情况,同时应用水均衡法与数值法对在不同东西边界条件下趵突泉泉域的水均衡进行了计算分析,两种方法互为验证,证明地下水均衡计算结果较为准确。

(1)在断裂-分水岭作为趵突泉泉域边界时,需要考虑地表水与地下水之间密切的水力联系以及两者之间的转化关系。通过建立断裂-分水岭区域的数值模型,初步建立河道排泄量占比(R_{SR})、孔隙水

出流量占比(R_{PSSR})、裂隙水出流量占比(R_{KSSR})与降水量 P 的关系。河道排泄量占比与降水量的相关关系为 $R_{SR} = 33.967 \ln P - 14.728$,裂隙水出流量占比与降水量 P 的相关关系为 $R_{KSSR} = -30.52 \ln P + 59.941$,孔隙水出流量占比约为 50%。合理折算各部分水量,可以提高水均衡计算结果的准确性。

(2)在上述认识的前提下,对在两种边界条件下的趵突泉泉域进行水均衡分析。对于同一种边界的泉域水均衡情况,两种方法计算结果接近,表明水均衡计算结果较为准确。根据水量均衡法和数值法计算结果,断裂边界泉域的补给量、排泄量以及均衡差均大于断裂-分水岭边界泉域。断裂边界泉域均衡差分别比断裂-分水岭边界泉域大 564.6 万 m^3/a 和 767.5 万 m^3/a ,表明在不同边界条件下泉域水均衡情况存在一定差异,但差距较小。

目前对趵突泉泉域边界尚无统一认识,断裂-分水岭边界是基于近些年的野外水文地质补充勘察结果提出的,但目前对断裂-分水岭边界的研究较少,为了名泉保护与供水的双重需要,有必要对趵突泉泉域的边界展开深入研究。需要重视数据的时效性,结合钻孔资料、水位资料,利用水动力学法、水化学法等多种方法提供佐证,得到关于趵突泉泉域边界的准确答案。

参考文献(References):

[1] BONACCI O. Ground water behaviour in karst; example of the Ombla spring (Croatia)[J]. Journal of Hydrology, 1995, 165(1/4): 113-134. DOI: 10. 1016/0022-1694(94)02577-X.

[2] 徐中平,周训,崔相飞,等.岩溶区地下水数值模拟研究进展[J].中国岩溶,2018,37(4):475-483. (XU Z P, ZHOU X, CUI X F, et al. Advances in numerical simulation of groundwater in karst areas[J]. China Karst, 2018, 37(4): 475-483. (in Chinese)) DOI: CNKI: SUN;

- ZGYR, 0. 2018-04-001.
- [3] 束龙仓,朱元甦,孙庆义,等. 地下水资源评价结果的可靠性探讨[J]. 水科学进展, 2000, 11(1): 21-24. (SHU L C, ZHU Y S, SUN Q Y, et al. Discussion on the reliability of evaluation results of groundwater resources [J]. Progress in Water Science, 2000, 11(1): 21-24. (in Chinese)) DOI: 10. 14042/j. cnki. 32. 1309. 2000. 01. 004.
- [4] 束龙仓,朱元甦. 地下水资源评价中的不确定性因素分析[J]. 水文地质工程地质, 2000(6): 6-8. (SHU L C, ZHU Y S. Analysis of uncertain factors in groundwater resource evaluation[J]. Hydrogeology and Engineering Geology, 2000 (6): 6-8. (in Chinese)) DOI: 10. 3969/j. issn. 1000-3665. 2000. 06. 002.
- [5] 陈晓宏,颜依寒,李诚,等. 溶蚀丘陵型岩溶流域概念性水文模型及其应用[J]. 水科学进展, 2020(1): 1-9. (CHEN X H, YAN Y H, LI C, et al. Conceptual hydrological model for karst hilly karst watershed and its application [J]. Advances in Water Science, 2020 (1): 1-9. (in Chinese)) DOI: 10. 14042/j. cnki. 32. 1309. 2020. 01. 001.
- [6] 赵春红,李强,梁永平,等. 北京西山黑龙关泉域岩溶水系统边界与水文地质性质[J]. 地球科学进展. 2014, 29(3): 412-419. (ZHAO C H, LI Q, LIANG Y P, et al. Karst water system boundaries and hydrogeological properties of Heilongguan springshed in Xishan Region, Beijing [J]. Advances in Earth Science, 2014, 29(3): 412-419. (in Chinese)) DOI: 10. 11867/j. issn. 1001-8166. 2014. 03. 0412.
- [7] 白媛丽. 柳林泉域岩溶水系统特征及泉流量动态模拟研究[D]. 太原: 太原理工大学, 2012. (BAI Y L. Study on characteristics of karst water system and spring flow dynamic simulation in Litulin Spring region [D]. Taiyuan: Taiyuan University of Technology, 2012. (in Chinese)) DOI: 10. 7666/d. y2156053.
- [8] 申豪勇,梁永平,赵春红,等. 古堆泉岩溶地下水系统特征及系统圈划[J]. 吉林大学学报(地球科学版), 2020, 50(1): 219-227. (SHEN H Y, LIANG Y P, ZHAO C H, et al. Characteristics and system circle of Gudui spring karst groundwater system [J]. Journal of Jilin University (Earth Science edition), 2020, 50(1): 219-227. (in Chinese)) DOI: 10. 13278/j. cnki. jjuese. 20180281.
- [9] 梁永平,王维泰. 中国北方岩溶水系统划分与系统特征[J]. 地球学报, 2010, 31(6): 860-868. (LIANG Y P, WANG W T. Classification and system characteristics of karst water systems in northern China [J]. Journal of Earth, 2010, 31(6): 860-868. (in Chinese)) DOI: 10. 3975/cagsb. 2010. 06. 10.
- [10] 侯光才,林学钰,苏小四,等. 鄂尔多斯白垩系盆地地下水系统研究[J]. 吉林大学学报(地球科学版), 2006, 36(3): 391-397. (HOU G C, LIN X Y, SU X S, et al. Research on groundwater system of Cretaceous basin in Ordos [J]. Journal of Jilin University (Earth Science edition), 2006, 36(3): 391-397. (in Chinese)) DOI: 10. 3969/j. issn. 1671-5888. 2006. 03. 013.
- [11] 王波,张华,王宇,等. 泸西喀斯特断陷盆地地表水与地下水流域边界与水动力性质[J]. 中国岩溶, 2020, 39(3): 319-326. (WANG B, ZHANG H, WANG Y, et al. Watershed boundary and hydrodynamic properties of surface water and groundwater in Luxi Karst Fault basin [J]. China Karst, 2020, 39(3): 319-326. (in Chinese)) DOI: 10. 11932/karst20200302.
- [12] 倪寒茜,束龙仓,韩刚,等. 城市化对趵突泉泉域降水入渗补给的影响[J]. 南水北调与水利科技(中英文), 2020, 18(6): 60-70, 147. (NI H X, SHU L C, HAN G, et al. Impact of urbanization on precipitation infiltration recharge in Baotu Spring basin [J]. South-to-North Water Transfers and Water Science & Technology, 2020, 18(6): 64-70, 147. (in Chinese)) DOI: 10. 13476/j. cnki. nsbdqk. 2020. 0115.
- [13] 邢立亭,李常锁,周娟,等. 济南泉域岩溶径流通道特征[J]. 科学技术与工程, 2017, 17(17): 57-65. (XING L T, LI C S, ZHOU J, et al. Characteristics of karst runoff channels in Jinan Spring basin [J]. Science, Technology and Engineering, 2017, 17(17): 57-65. (in Chinese)) DOI: CNKI: SUN: KXJS. 0. 2017-17-005.
- [14] 孟庆晗,王鑫,邢立亭,等. 济南四大泉群补给来源差异性研究[J]. 水文地质工程地质, 2020(1): 37-45. (MENG Q H, WANG X, XING L T, et al. Study on the difference of the supply sources of four spring groups in Jinan [J]. Hydrogeology and Engineering Geology, 2020 (1): 37-45. (in Chinese)) DOI: 10. 16030/j. cnki. issn. 1000-3665. 201906014.
- [15] 孙斌,彭玉明,李常锁,等. 济南岩溶水系统划分及典型泉域水力联系[J]. 山东国土资源, 2016(10): 31-34, 38. (SUN B, PENG Y M, LI C S, et al. Jinan karst water system division and typical spring hydraulic connection [J]. Shandong Land and Resources, 2016 (10): 31-34, 38. (in Chinese)) DOI: 10. 3969/j. issn. 1672-6979. 2016. 10. 007.
- [16] 奚德荫,李祥芝,邵卓,等. 山东省济南市保泉供水水文地质勘探水质模型报告[R]. 山东省地矿局 801 水文地质工程地质大队, 1989. (XI D Y, LI X Z, SHAO Z, et al. Hydrogeological exploration report of spring protection and water supply in Jinan City, Shandong Province [R]. Shandong Provincial Bureau of Geology and Mineral Resources 801 Hydrogeology and Engineering Geology Brigade, 1989. (in Chinese))

- [17] 董咏梅, 苏光星, 李占华. 从济西抽水试验探济南泉域西边界[J]. 水资源保护, 2004, 20(3): 58-59. (DONG Y M, SU G X, LI Z H. The western boundary of Jinan Spring basin was explored by pumping test in Jixi[J]. Water Resources Protection, 2004, 20(3): 58-59. (in Chinese)) DOI: 10. 3969/j. issn. 1004-6933. 2004. 03. 019.
- [18] 孙斌, 彭玉明. 济南泉域边界条件、水循环特征及水环境问题[J]. 中国岩溶, 2014, 33(3): 272-279. (SUN B, PENG Y M. Boundary conditions, water cycle characteristics and water environment problems in Jinan Spring basin[J]. China Karst, 2014, 33(3): 272-279. (in Chinese)) DOI: CNKI; SUN; ZGYR. 0. 2014-03-003.
- [19] 王建军. 济南岩溶区地下水系统数值模拟及保泉供水管理模型研究[D]. 济南: 山东大学, 2016. (WANG J J. Numerical simulation of groundwater system in Jinan karst area and study on the management model of spring water conservation [D]. Jinan: Shandong University, 2016. (in Chinese)) DOI: 10. 7666/d. Y3156516.
- [20] 祁晓凡, 李文鹏, 李海涛, 等. 济南岩溶泉域地下水位、降水、气温与大尺度气象模式的遥相关[J]. 水文地质工程地质, 2015, 42(6): 18-28. (QI X F, LI W P, LI H T, et al. Remote correlation between groundwater level, precipitation, air temperature and large-scale meteorological model in Jinan karst spring region [J]. Hydrogeology and Engineering Geology, 2015, 42(6): 18-28. (in Chinese)) DOI: 10. 16030/j. cnki. issn. 1000-3665. 2015. 06. 04.
- [21] 杨丽芝, 李壮, 卫政润, 等. 济南城市地质调查报告[R]. 山东省地质调查院, 2014. (YANG L Z, LI Z, WEI Z R, et al. Urban geology survey report of Jinan [R]. Shandong Institute of Geological Survey, 2014. (in Chinese))

Analysis of water balance in Baotu Spring basin under two typical boundary conditions

SHU Longcang¹, ZHANG Manqi¹, LI Hu², NI Hanxi¹, WU Zhaojun², CHEN Yuan¹, WANG Xiaobo¹, YU Yafei¹

(1. College of Hydrology and Water Resources, Hohai University, Nanjing 210098, China;

2. Jinan Rail Transit Group Co. Ltd, Jinan 250014, China)

Abstract: Accurate understanding of groundwater balance in karst area can provide technical guarantee for scientific evaluation of groundwater resources. To study the water balance in karst area, it is necessary to clarify the boundary conditions and hydrogeological properties of karst water system. However, due to the high complexity of geological structures and karstic development in the karstic area, it has become one of the difficult problems in current research. The Baotu Spring basin is a typical karst basin in northern China. At present, there are two different views on the east and west boundaries of the Baotu Spring basin. If the boundary of the Baotu Spring basin is unclear and its hydrogeological property is unknown, the calculation of water balance in the Baotu Spring basin can not be correctly carried out. The research on the boundary conditions and the water balance of Baotu Spring basin under two kinds of boundary conditions were carried out.

The main difference between the east and west boundaries is the area surrounded by the fault and the watershed, and the main recharge is the infiltration from precipitation. According to the actual hydrogeological conditions in the study area, a numerical model is established to simulate the conversion from precipitation to different types of runoff in the fault-watershed area to obtain its water exchange law. According to the obtained conversion law, the water balance method is used to calculate the replenishment and discharge in the study basin, and the water balance results of the two boundary conditions are obtained. On the other hand, based on the same law of water exchange, combining with the exploration data and drilling data of the Baotu Spring basin, the numerical simulation models of fault-boundary spring basin and fault-watershed boundary spring basin are established by the FEFLOW software, and the water balance of the two kinds of boundary conditions is calculated. The calculation results provided by the water-balance method and numerical simulation model are compared and analyzed.

Based on the numerical model of the fault-watershed area, the relationship between the precipitation and the proportion of surface runoff (SR/P), the proportion of porous subsurface runoff (PSSR/P), the proportion of karstic subsurface runoff (KSSR/P) can be established. The results provided by the numerical simulation model show that the relation between the proportion of surface runoff and precipitation is $R_{SR} = 33.967 \ln P - 14.728$, the relation between the proportion of karstic subsurface runoff and precipitation is $R_{KSSR} = -30.52 \ln P + 59.941$, and the proportion of porous subsurface runoff is about 0.50. Applying this law to the water-balance method, it is found that the replenishment, discharge and balance difference of the fault-boundary spring basin are respectively 9.022 million m^3/a , 3.376 million m^3/a and 5.646 million m^3/a larger than that of the fault-watershed boundary spring basin. Applying this law to the numerical simulation method, it is found that the replenishment, discharge and balance difference of the fault-boundary spring basin are all greater than that of the fault-watershed spring basin, and the difference values are 12.108 million m^3/a , 4.433 million m^3/a and 7.675 million m^3/a , respectively.

(下转第 445 页)

lems, such as small per capita water resource and large water consumption in food production and energy exploitation. However, the issue of water resource shortage is becoming more and more serious. To promote the sustainable development of resource, it is of practical significance to carry out the harmonious evaluation of water-energy-food coupling system and to study its changing relationship.

To evaluate the multi-dimensional coupling system harmoniously, and to reduce the uncertainty of each index from the incomplete data and the subjectivity of evaluation index selection, a comprehensive evaluation index system of water resource, energy, and food based on the harmonious quantification model is proposed. It couples the fuzzy multi-attribute decision-making method with the harmonious quantization method, and the harmonious degree of the water-energy-food coupling system is determined according to the weight of fuzzy language and the harmonious quantification. In addition, the data of Henan Province from 2011 to 2018 are selected to analyze the development level and harmony degree of water-energy-food coupling system, and explore the spatio-temporal variation characteristics of each subsystem and the coupling system.

During the study years, the harmony degree of water-energy-food coupling system in the whole province increases annually. In the study years, the improvement of harmony degree in the early stage is mainly affected by the energy system, while the later stage is related to the food system and water resource system. The development characteristics of each subsystem are different, but the whole system presents an upward trend. Due to the improvement of water use efficiency, and the remarkable effect of pollution control, the harmony degree of water resource system fluctuates, which indicates that the state of water resource in Henan Province continues to improve. The harmony degree of the energy system reached the maximum in 2015, and the harmony degree is the best. However, with the change of industrial structure, the total power of rural machinery decreased, and with the increase of urban electricity consumption, the harmony degree of the system become worse, and the overall trend of change is upward, fluctuating, and downward. Because of the upgrading of agricultural technology, the increase of effective irrigation area and other factors, the harmony degree of food system shows a gradual upward trend, and reach the maximum value in 2018.

In general, the harmony degree of water resource system in Henan Province is the highest, followed by the food system and the energy system. The food subsystem has a relatively high development level and stable performance, while the energy subsystem has a fluctuating development and poor stability. The harmonious quantization method based on fuzzy multi-attribute decision-making can solve the uncertainty problem in index quantization. Meanwhile, the results can account for complex information and recognize the subtle differences between the indicators, making it easier for decision makers to identify the adverse development factors. The harmonious evaluation of the comprehensive system can support the management of water resource, energy and food system.

Key words: water-energy-food coupling system; harmony quantization; spatio-temporal evolution; Henan Province

(上接第 436 页)

The precipitation in the fault-watershed region is converted into surface runoff (SR), porous subsurface runoff (PSSR) and karstic subsurface runoff (KSSR) runoff in a certain proportion. Therefore, when the fault-watershed is used as the boundary of the Baotu Spring basin, it is necessary to consider the close hydraulic relationship between surface water and groundwater as well as the transformation relationship between them. Reasonable conversion of the water volume of each part can improve the accuracy of water balance calculation results. Combining with the law of water exchange in the fault-watershed region, the water balance in the spring basin is calculated by the traditional water balance method and the numerical simulation method. The calculation results of the two methods show that the replenishment, discharge and balance difference of the fault boundary spring basin are greater than that of the fault-watershed boundary spring basin. There are some differences in spring water balance under different boundary conditions, but the difference is small.

Key words: karst springs basin; boundary condition; water balance; numerical method